

P. Ola G. Persson¹, Christopher W. Fairall², Edgar L Andreas³, and Peter S. Guest⁴

¹Cooperative Institute for Research in Environmental Sciences/NOAA/ETL, Boulder, CO

²NOAA/Environmental Technology Laboratory (ETL), Boulder, CO

³Army Cold Regions Research and Engineering Laboratory (CRREL), Hanover, NH

⁴Naval Postgraduate School (NPS), Monterey, CA

1. INTRODUCTION

Though measurements of some components of the surface energy budget of the Arctic pack ice have been made previously, notably at the Soviet ice stations (NSIDC 1996), no adequate direct observations of all components of the surface energy budget at one location in the pack ice throughout an entire annual cycle have been made. Therefore, in surface energy budget studies (e.g., Maykut and Untersteiner, 1971 (MU71); Maykut, 1982 (M82); Ebert and Curry, 1993 (EC93); Lindsay, 1998 (L98); Jordan *et al.*, 1999), some or all of the fluxes are computed using parameterizations with uncertain accuracies.

This paper presents observations of surface energy budget terms during the Surface Heat Budget of the Arctic Ocean Experiment (SHEBA) (Perovich *et al.*, 1999) as represented by the Atmospheric Surface Flux Group (ASFG) data set (Andreas *et al.*, 1999). Persson *et al.* (2001a,b) provide descriptions of the ASFG site, instruments, and data processing, along with estimates and examples of data accuracy. Hence, these topics will not be addressed here. The data is unique because it provides direct measurements of all components of the surface energy budget except conduction with hourly resolution throughout nearly an entire annual cycle. Comparisons to previous surface energy studies in the Arctic provide a context for understanding the significance of the various terms.

2. THE SURFACE ENERGY BUDGET

We will consider a surface slab of finite thickness consisting of snow during most of the year and ice with melt ponds during the summer, similar to that within view of the ASFG radiometer (see photos in Persson *et al.* 2001a). The total energy flux, F_{tot} , into this surface slab is given by

$$F_{\text{tot}} = Q^* - H_s - H_l + C, \quad (1)$$

where Q^* is the total net radiative flux, H_s is the sensible heat flux, H_l is the latent heat flux and C is the conductive flux. Q^* is given by

$$Q^* = Q_s + Q_l = Q_{s_i} - Q_{s_o} + Q_{l_i} - Q_{l_o} = Q_{s_i}(1 - \alpha) + Q_l, \quad (2)$$

where Q_s is the net solar radiation, Q_l the net longwave radiation, Q_{s_i} the incoming solar radiation, Q_{s_o} the outgoing solar radiation, Q_l the incoming longwave radiation, Q_{l_o} the outgoing longwave radiation, and α

the surface albedo. Because (2) assumes that all radiative flux is absorbed within this surface slab, it overestimates the energy input from above during July and August when a monthly average of 1-7 Wm^{-2} of solar energy penetrates through the ice into the ocean.

H_s was measured by the covariance method on the 20-m ASFG meteorological tower. To increase the number of data points, the median value of H_s from the five tower levels for each hour is used. Though H_l was directly measured through covariance techniques at one level, its bulk estimate at 10 m (H_{l_b}) is used in the calculations presented here. Using H_{l_b} rather than H_l increases the latent heat flux during May and June by 2 Wm^{-2} and 5 Wm^{-2} , respectively, but makes no significant difference during the other months.

While a snow cover is present (October-June), C is estimated from the temperature gradient in the snowpack obtained from the ice/snow interface temperature (T_{ice}), the best radiative estimate of the surface temperature (T_s), manual snow depth measurements (d_s) at the ASFG site and the relation

$$C = -k_s [(T_s - T_{\text{ice}})/d_s]. \quad (3)$$

Two values for the thermal conductivity of the snow (k_s) are used. The first value ($0.14 \text{ W m}^{-1} \text{ K}^{-1}$) was obtained with conductivity probe measurements by Sturm *et al.* (2001) in the vicinity of the SHEBA site in April. We also use a more standard value of $k_s = 0.3 \text{ W m}^{-1} \text{ K}^{-1}$, since Sturm *et al.* (2001) show that their direct measurement of k_s is unusually low and inconsistent with the observed wintertime bottom accretion of ice and evolution of the temperature profiles in the ice and snow. This gives a range for C . Because of a spatial separation of the radiative surface temperature and the snow depth measurements and a spatial difference in snow depth, the conductive fluxes obtained from the ASFG site are considered coarse estimates.

During times with no snow cover, the conductive flux is calculated using the water temperature at the bottom of the ice ($T_w = -1.8^\circ \text{C}$), the ice thickness ($d_i = 2.0 \text{ m}$), the thermal conductivity of the ice ($k_i = 2.0 \text{ W m}^{-1} \text{ K}^{-1}$), and

$$C = -k_i [(T_s - T_w)/d_i]. \quad (4)$$

All terms on the right-hand sides of (1) and (2) are directly measured at the ASFG site except C , which is calculated from (3) or (4). Daily and monthly means were calculated from hourly values of each energy budget term.

F_{tot} at a given time may be positive, negative, or zero. If F_{tot} is positive, the snow or ice gains energy, which can be used to either increase its temperature, or if the temperature is already at the melting point, to produce melting. If F_{tot} is negative, the surface slab loses energy and the slab temperature decreases. Only

Corresponding author address: Dr. Ola Persson, R/ET7, NOAA/ETL, 325 Broadway, Boulder, CO 80305; opersson@etl.noaa.gov

the change of phase in this surface slab is included, and not the change of phase at the bottom of the ice. About 0.70 m of ice melted from the top of the undeformed multi-year ice pack during the year (Perovich *et al.*, 1999) along with about 0.5 m of snow estimated for the ASFG radiometer site (equivalent to about 0.18 m of ice). A net of 0.35 m of ice grew on the bottom of the ice (Perovich *et al.* 1999). The first two values imply an expected net energy flux excess in the surface slab, and the latter a deficit at the bottom of the ice.

3. ANNUAL CYCLE

Monthly mean surface energy budget values for the ASFG site are presented here and are compared to the earlier studies, which generally also use monthly means. However, each surface energy budget term shows large day-to-day variability. Large variability in Q_l and Q_s were related to the presence of clouds, while large peaks (in magnitude) of H_s and H_l often correspond to a synoptic event that has increased the wind speed. Persson *et al.* (1999a,b; 2001b) discuss this high-frequency variability in more detail.

The monthly means show a net flux energy deficit of 10-20 Wm^{-2} from September through March and an energy surplus from April to August (Fig. 1a), with a peak of about 80 Wm^{-2} in July. (The October 1998 value was interpolated from September 1998 and November 1997 values.) Clearly, the radiative terms are dominant (Fig. 1b). The net shortwave has a positive impact from March to September, and the net longwave radiation is negative throughout the year, resulting in a positive net radiation balance from May through August and a negative balance during September through March. Though a factor 5-10 smaller in magnitude, the average turbulent heat flux ($H_s + H_{lb}$) opposes the effect of the net radiation, except during July. That is, it warms the surface during the winter and July while cooling it slightly during May, June, and August. The July downward H_s results from warmer air aloft being present over a surface with a fixed temperature of 0°C. Both of our estimates of the conductive flux have magnitudes comparable to the turbulent heat flux, warm the surface during the winter, and have little effect during the summer.

Figure 1a shows the running mean of the net flux from November 1997 to October 1998. By October 1998, an annual average energy excess of 6.0-8.6 Wm^{-2} exists, with the smaller and larger values corresponding to the use of the smaller and larger values of the thermal conductivity, respectively. This annual excess corresponds to a net melt of 0.72-1.03 m of ice. Hence, the estimated excess energy in the surface slab and the observed surface melt of 0.88 m ice equivalent agree well.

4. COMPARISONS TO PREVIOUS STUDIES

Because the SHEBA estimate of the annual cycle of the surface energy budget is based entirely on flux measurements, comparisons with budgets from other studies using climatological data, models, and parameterizations could reveal differences leading to new interpretations of the energy budget over the Arctic pack ice and insights into possible model shortcomings.

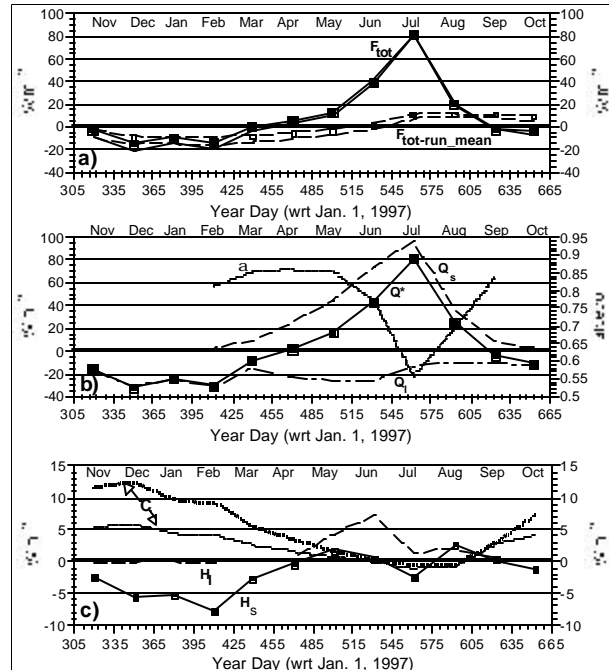


Fig. 1: Surface energy budget using monthly means. The terms are a) F_{tot} (solid) and the cumulative mean of F_{tot} beginning on November 1, 1997 (dashed); b) Q_s (grey solid), Q^* (dotted), Q (dark solid), and a (dot-dash); and c) H_s (solid), H_{lb} (dashed), and C (dotted). In a) and c), both $k_s = 0.14 W m^{-1} K^{-1}$ (thin lines) and $k_s = 0.3 W m^{-1} K^{-1}$ (thick lines) are used for determining C .

The studies of MU71, M82, EC93, and L98 are used here for comparisons. MU71 was a modeling study over a uniform multi-year ice pack using climatological forcing parameters. L98 used Soviet drifting ice station data to derive forcing parameters and then used parameterizations to compute surface fluxes. Because the ice stations were located on multi-year ice floes, this study probably did not include substantial effects of leads. In contrast, the modeling study by M82 partitioned the pack ice into thickness categories, including leads, to obtain integrated surface fluxes. The 1-D model of EC93 included the effects of melt ponds and leads as well as sophisticated parameterizations of some parameters such as albedo. Because the SHEBA ASFG site was on a 1.9-m-thick multi-year floe and leads were not directly sampled by the observations, we expect that the surface energy budget at the ASFG site is more similar to the conditions in the studies of MU71 and L98 than to those in M82 and EC93, though some effects from the nearby melt pond at the ASFG site were measured.

Comparisons of net radiation throughout the annual cycle (Fig. 2a) show that the SHEBA Q^* was generally comparable to the climatological (M82) and parameterized (L98) fluxes, though there are differences of up to 30 Wm^{-2} for some individual months (e.g., August compared to M82). However, despite the agreement in Q^* , some notable differences exist in individual radiative components. Note first that, despite the SHEBA July Q^* occurring between the two other studies, the albedo for July at SHEBA is 0.10 lower. However, the incoming shortwave radiation at SHEBA in

midsummer is $25\text{-}50\text{ Wm}^{-2}$ lower than the other studies (Fig. 2b), explaining why a comparable net shortwave radiation and net Q^* are obtained with a lower albedo. Recall that the ASFG albedo shown here includes the effect of a melt pond during July and is similar to the Ice Physics group (IPG) albedo-line average (see Persson *et al.* 2001a).

More downward longwave radiation occurred at SHEBA during March and April (Fig. 2c) than for the other studies, possibly indicating the occurrence of more springtime clouds and/or warmer atmospheric temperatures at SHEBA. The SHEBA floe's spring location in the Chukchi Sea just north of the Bering Strait may also have favored clouds compared to other regions in the Arctic Basin. Interestingly, the incoming shortwave radiation at SHEBA isn't significantly lower during these two months, and the net radiation is only slightly higher for March and is comparable for April (Fig. 2a). The surface temperature was abnormally high at SHEBA during these two months (not shown), so the outgoing longwave radiation was unusually large, resulting in a Q_l comparable to the other studies.

The observed SHEBA turbulent heat fluxes have an annual cycle similar to the previous studies, except that the summer fluxes are $5\text{-}10\text{ Wm}^{-2}$ lower (Fig. 2d,e). There is slightly better agreement with L98 than with M82, especially since L98 shows a tendency for H_s to warm the surface in July. Note that the smaller SHEBA values imply that the atmosphere doesn't cool the surface as much, permitting more surface heating and melting. Our crude estimate of the SHEBA winter conductive flux is $5\text{-}15\text{ Wm}^{-2}$ less than that used in the previous studies (Fig. 2f). This comparison may change by using the improved estimates from the IPG data.

For the total annual budget, the SHEBA-ASFG data show 6-11% less incoming solar radiation than the other studies (Table 1). However, because of the lower albedo, the net solar radiation is similar to MU71 and L98 but still lower than M82 and EC93. The ASFG data

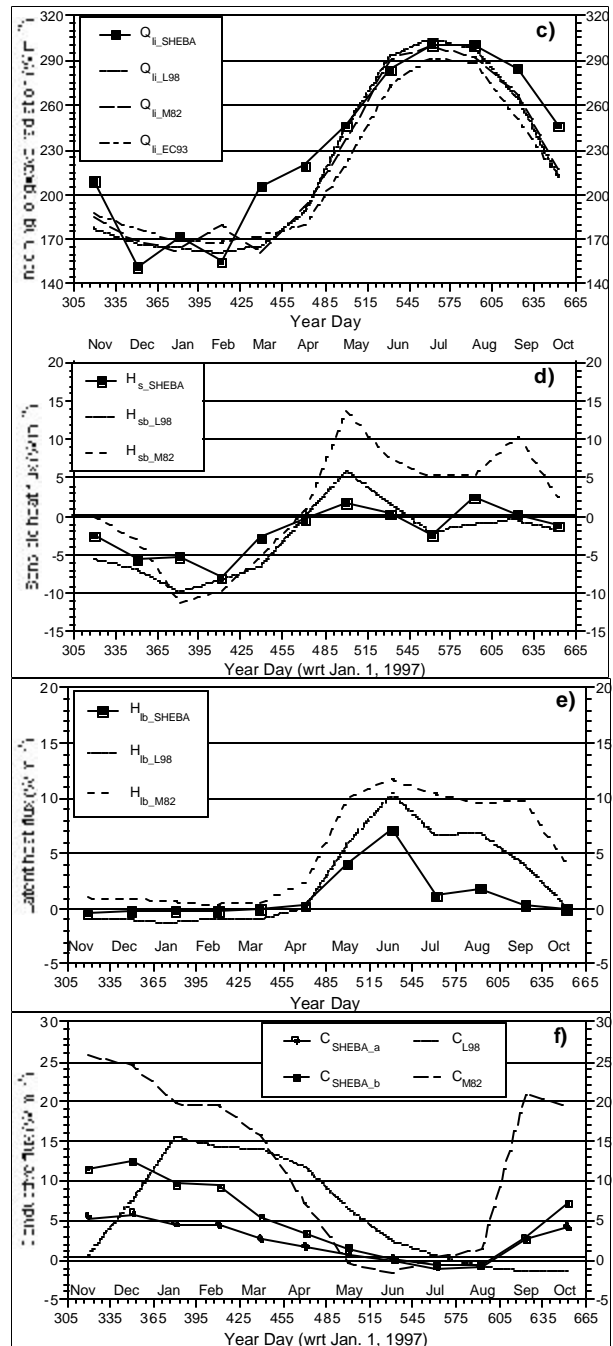
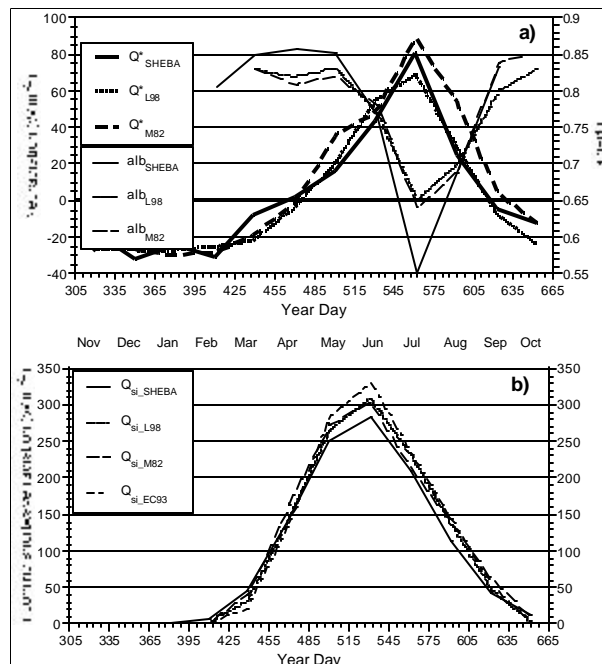


Fig. 2: Comparisons of selected SHEBA monthly mean surface energy budget components with previous studies. Shown are a) net radiation (Q^* ; heavy lines) and albedo (thin lines), b) incoming shortwave radiation (Q_{si}), c) incoming longwave radiation (Q_{li}), d) sensible heat flux (H_s), e) latent heat flux (H_{lb}), and f) conductive flux (C). The previous studies used in the comparisons are M82(dashed), L98 (dotted), and EC93 [dash-dot in b) and c) only]. In f), SHEBA curves are shown using C determined from $k_s = 0.14\text{ W m}^{-1}\text{ K}^{-1}$ (thin line) and $k_s = 0.3\text{ W m}^{-1}\text{ K}^{-1}$ (thick line).

Table 1: Comparison of annual energy budget components from the SHEBA observations with MU71, M82, EC93, and L98. Values are given as annual average fluxes (Wm^{-2}). C and F_{tot} in column two use $k_s = 0.14 W m^{-1} K^{-1}$ ($0.3 W m^{-1} K^{-1}$)

Term	SHEBA -ASFG	MU71	M82	EC93	L98
Q_{si}	90.9	100.0	100.0	101.3	96.8
Q_s	24.1	24.2	29.6	29.5	23.2
Q_{lj}	230.4	220.2	220.2	215.3	219.3
Q_l	-21.3	-24.4	-22.3	-28.4	-22.7
H_s	-2.0	-3.6	1.3	-1.8	-3.0
H_{lb}	1.1	4.2	5.0	1.6	2.3
$Q_s + Q_l - H_s - H_{lb}$	3.7	-0.9	0.9	1.3	1.2
C	2.3 (4.8)	8.0	12.5	8.1	5.7
F_{tot}	6.0 (8.6)	7.0	13.4	9.4	6.9

show 10-15 Wm^{-2} more incoming longwave radiation and a 1-7 Wm^{-2} smaller net longwave radiation loss. The observed sensible heat flux is similar to estimates by EC93 and L98, but the observed latent heat flux is substantially less than all but EC93. The most significant differences are seen when comparing the sums of the atmospheric fluxes ($Q_s + Q_l - H_s - H_{lb}$), for which the ASFG data show a much larger excess than that shown by the other studies (MU71 has a small deficit). Because the conductive flux is smaller for the ASFG data, the observed annual energy excess in the surface layer is similar to that predicted by three of the four other energy budget estimates.

Accounting for known errors and further processing of the ASFG data set, corrections of 03 Wm^{-2} are possible in F_{tot} producing an adjusted value in the 6-12 Wm^{-2} range. The observed ice/snow melt of 0.88 m ice equivalent at SHEBA implies an annual average surface energy flux excess of 8.4 Wm^{-2} . This value falls within both the original range from the observations presented here and that estimated for refinements to the data set.

If the annual average F_{tot} values of 6.9-7.0 Wm^{-2} from MU71 and L98 are representative of equilibrium conditions (the model in MU71 was run until equilibrium conditions were established; L98 used observations from 1957-1990) at a multi-year ice site such as the SHEBA site, the larger annual average energy flux excess of 8.4 Wm^{-2} estimated from the observed melt agrees qualitatively with the net loss of 0.35 m of ice (surface ablation minus bottom accretion) observed at SHEBA (Perovich *et al.*, 1999). Since the range of the observed SHEBA annual surface energy flux excess encompasses both the equilibrium-model values and the value from the observed melt, it will be necessary to improve the data set to the extent that it can differentiate between equilibrium conditions and the ice-loss conditions observed at SHEBA. This will not only require corrections of the radiometer cold and zenith angle biases and the latent heat flux biases due to the use of the bulk values, but will also require a significant reduction in the uncertainty of the conductive flux value.

5. CONCLUSIONS

Though the uncertainties in the data imply that the surface energy budget described here must be regarded

as preliminary, error estimates suggest that the relative importance of the various terms will not change qualitatively with future refinements. Nevertheless, climatologically important conclusions requiring further accuracy must await such refinements.

If the effective k_s truly is 0.3 $W m^{-1} K^{-1}$, as the results of Sturm *et al.* (2000) suggest, and the various corrections to the observed data make no substantial changes to the average annual flux excess given here, the observed annual average flux excess of 8.6 Wm^{-2} would be in remarkable agreement with the flux excess of 8.4 Wm^{-2} expected from the observed surface melt. We could then conclude that the SHEBA year produced a net melt because of the unusually large surface melt due to 1) greater incoming longwave radiation and 2) weaker cooling by the latent heat flux. Weaker warming by the sensible heat and conductive fluxes was inadequate to completely compensate. This conclusion is dependent on the above caveats and hence tentative.

6. REFERENCES

- Andreas, E. L., C. W. Fairall, P. S. Guest, and P. O. G. Persson, 1999. An overview of the SHEBA atmospheric surface flux program, *Preprints, Fifth Conf. On Polar Meteorology and Oceanography*, 10-15 Jan, Dallas, TX, Amer. Meteor. Soc., Boston, 411-416.
- Ebert, E. E., and J. A. Curry, 1993. An intermediate one-dimensional thermodynamic sea-ice model for investigating ice-atmosphere interactions, *J. Geophys. Res.*, 98, C6, 10,085-10,109.
- Jordan, R.E., E.L. Andreas, and A.P. Makshtas, 1999. The heat budget of snow-covered sea ice at North Pole 4, *J. Geophys. Res.*, 104, 7785-7806.
- Lindsay, R. W., 1998. Temporal variability of the energy balance of thick Arctic pack ice, *J. Clim.*, 11, 313-333.
- Maykut, G. A., 1982. Large-scale heat exchange and ice production in the Central Arctic, *J. Geophys. Res.*, 87, C10, 7971-7984.
- Maykut, G.A., and N. Untersteiner, 1971. Some results from a time-dependent thermodynamic model of sea ice, *J. Geophys. Res.*, 76, 1550-1575.
- National Snow and Ice Data Center, 1996. Arctic Ocean Snow and Meteorological Observations from Russian Drifting Stations. NSIDC, University of Colorado, Boulder, CO, CD-ROM. [Available from nsidc@kryos.colorado.edu]
- Perovich, D., and 22 others, 1999. Year on ice gives climate insights. *Eos, Trans., AGU*, 80 [41], 481-486.
- Persson, P. Ola G., C. W. Fairall, E. Andreas, P. Guest and D. Perovich, 2001a: Measurements near the Atmospheric Surface Flux Group tower at SHEBA Part I: Site description, data processing, and accuracy estimates. *J. Geophys. Res.* Submitted.
- Persson, P. Ola G., C. W. Fairall, E. Andreas, and P. Guest, 2001b: Measurements near the Atmospheric Surface Flux Group tower at SHEBA Part II: Near-surface conditions and surface energy budget. *J. Geophys. Res.* Submitted.
- Sturm, M., D. K. Perovich, and J. Holmgren, 2001. Thermal conductivity and heat transfer through the snow on the ice of the Beaufort Sea, *J. Geophys. Res.*, submitted